

Atomic data for astrophysics

Giulio Del Zanna
STFC Advanced Fellow
DAMTP, University of Cambridge UK

OUTLINE:

Some methods to measure chemical abundances in stellar coronae

Atomic data Calculations – e.g. **APAP Network (UK)**:

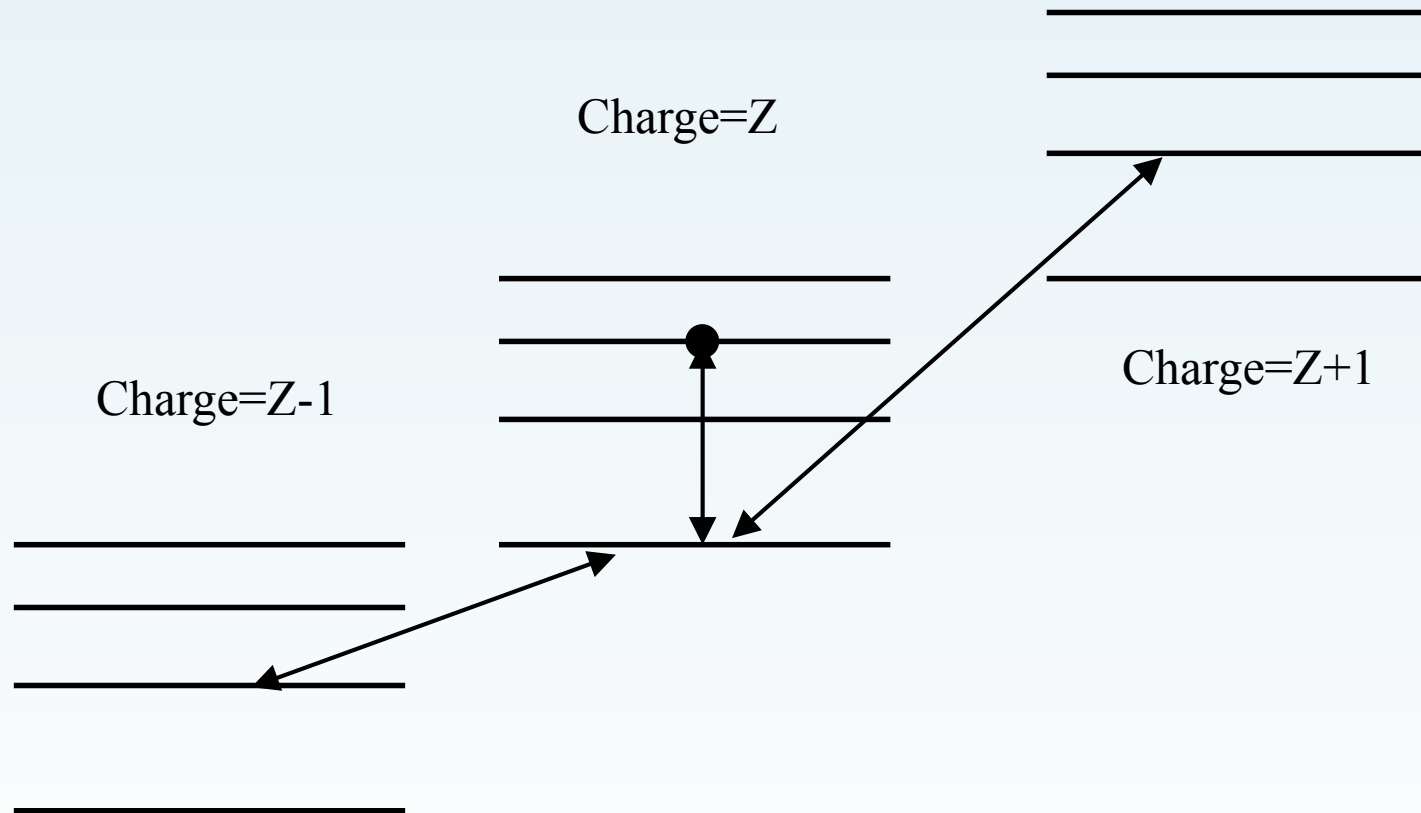
Benchmark of atomic data

Atomic Databases: **CHIANTI** and **VAMDC**

Ionization vs. excitation

Ionizations/recombinations occur on timescales of 1-100s

Dipole-allowed lines decay in 10^{-10} s. Forbidden ones in 10^{-4} s or longer



Treat separately excitation ionization

Intensities

- Separate excitation from ion/rec.

optically-thin plasmas line intensities are proportional to:

$$I \sim n_j A_{ji} = \frac{N_j(X^{+m})}{N(X^{+m})} A_{ji} \frac{N(X^{+m})}{N(X)} \frac{N(X)}{N(H)} \frac{N(H)}{N_e} N_e$$

Atomic data

Level population
(Ne, Te)

A-value

Ion
abundance
(Te, Ne)

El.
abundance

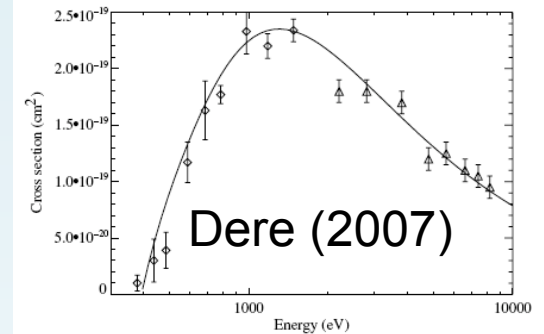
Measure:

Te, Ne, Abundances

Calculations of basic atomic data

1) Direct-ionization by electron impact:

Dere (2007) calculated ab-initio cross-sections of impact with ions and compared them with available experimental data for a large number of ions.



2) Radiative recombination: Badnell (2006).

3) Dielectronic recombination:

Badnell et al. (2003+ a number of papers).

4) R-matrix electron impact excitation:

1) Iron Project

2) STFC-funded (UK)

APAP Network <http://www.apap-network.org/>

atomic structure and e- scattering data for all astrophysically-important ions, sequence by sequence.

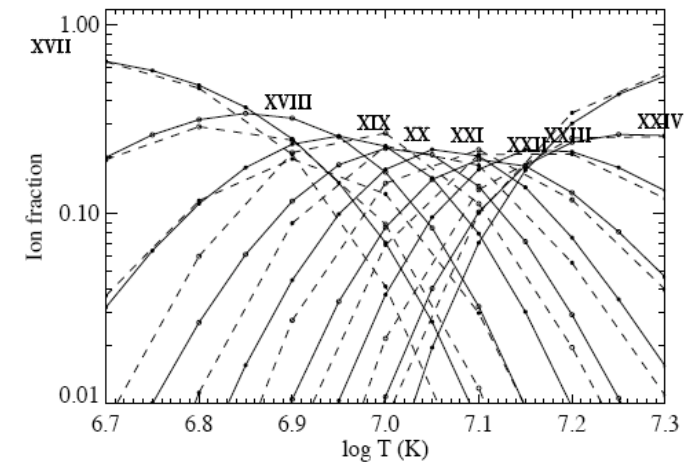


Fig. 3. Ionization equilibria for Fe XVII-XXIV. Full line - current calculations, dashed line = Mazzotta et al. (1998).



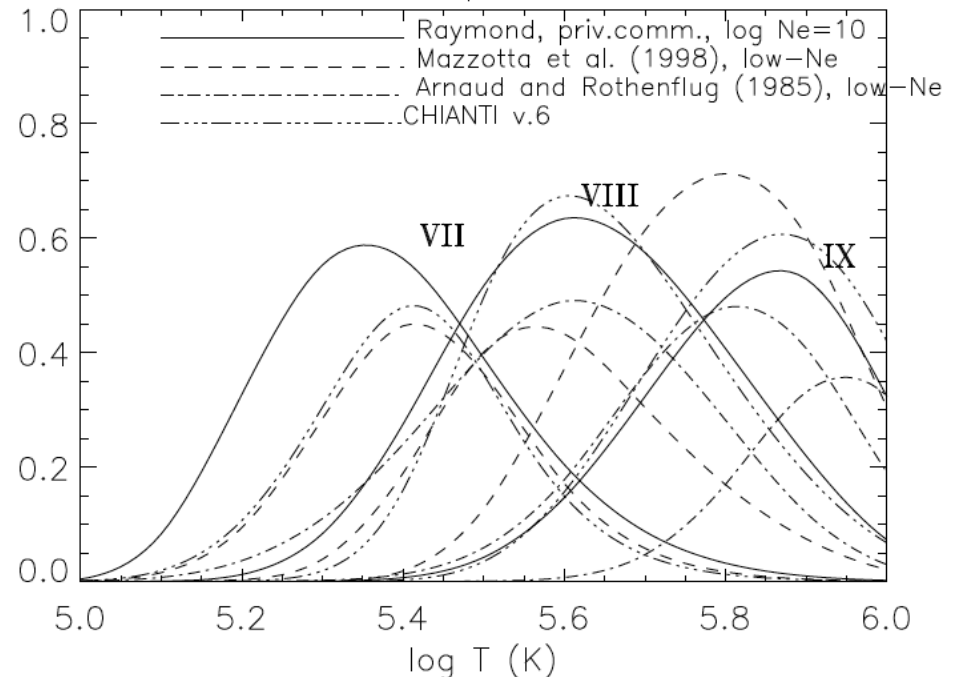
Ion abundances

Latest ion abundances are, for some ions, very different from previous ones.
Dere et al. (CHIANTI v6)

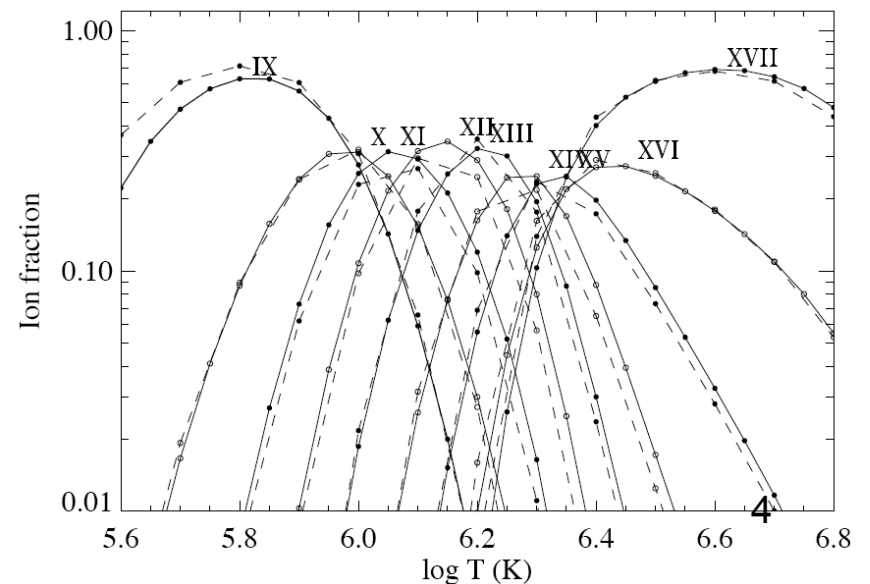
Time-dependent ionization can substantially affect spectral line intensities (e.g. Raymond, Noci, etc., see also Bradshaw, Del Zanna & Mason, 2003).

High densities affect ion abundances (Burgess & Summers 1969)

Ionization equilibria for Fe

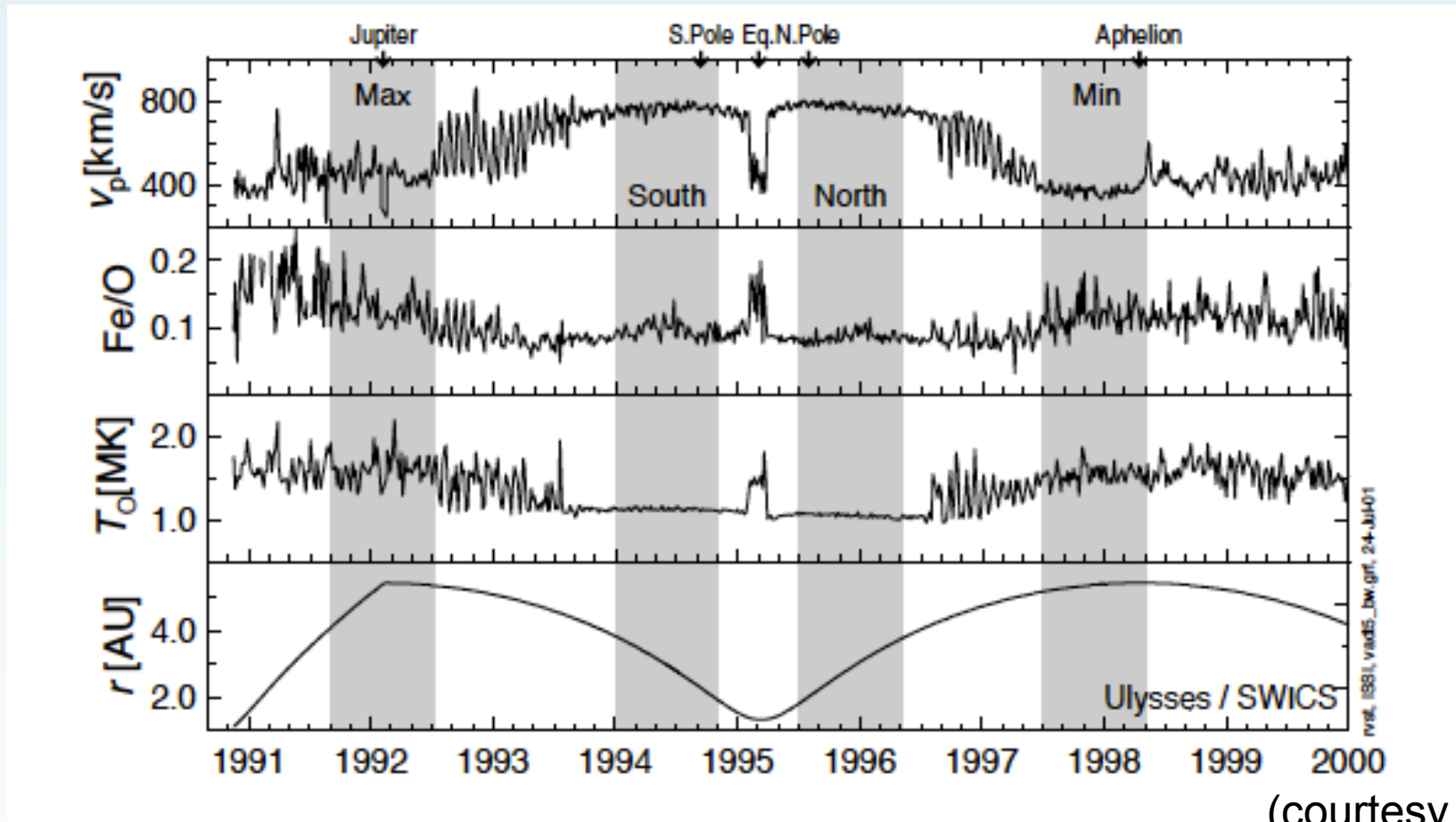


Del Zanna & Mason (2010)



In-situ measurements of the SW

Variation of low-FIP (e.g. Fe) vs. high-FIP (e.g. O) with solar wind.



(courtesy of R. von Steiger)

‘Canonical’ FIP bias was 4, now 2-3.
For some elements (Ar, Ne, He !) only ‘coronal’ values !

Intensities and EM/DEM

$$I(\lambda_{ij}) = \frac{h\nu_{ij}}{4\pi} \int N_j A_{ji} dh = \int Ab(X)C(T, \lambda_{ij}, N_e)N_eN_H dh \quad [\text{ergs cm}^{-2} \text{ s}^{-1} \text{ sr}^{-1}]$$

$$C(T, \lambda_{ij}, N_e) = \frac{h\nu_{ij}}{4\pi} \frac{A_{ji}}{N_e} \frac{N_j(X^{+m})}{N(X^{+m})} \frac{N(X^{+m})}{N(X)} \quad [\text{ergs cm}^3 \text{ s}^{-1}]$$

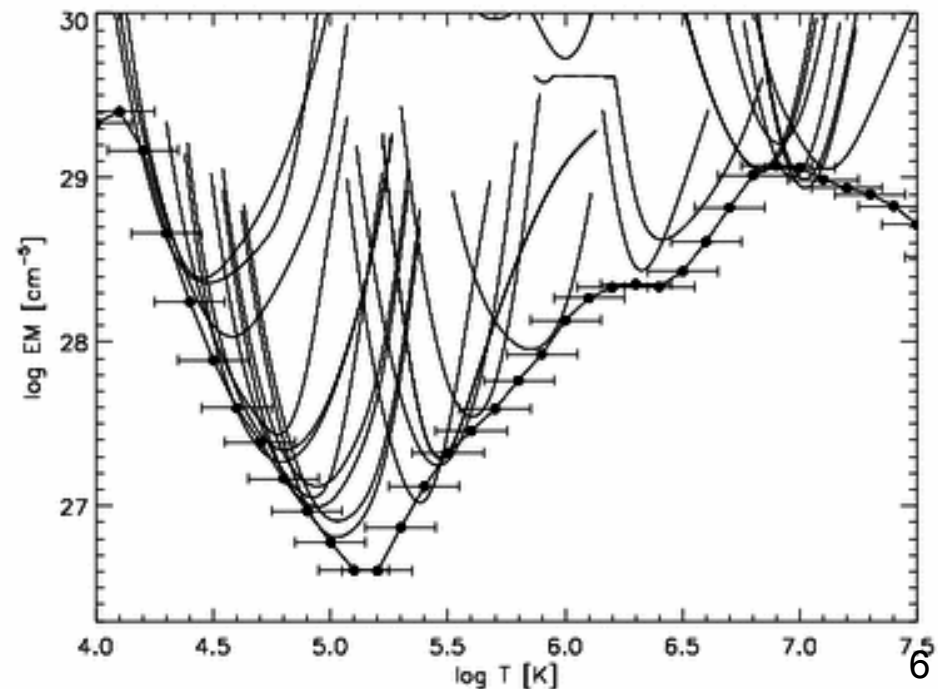
$$\text{DEM}(T) \equiv N_e N_H \frac{dh}{dT} \quad [\text{cm}^{-5} \text{K}^{-1}]$$

$$\text{EM} \equiv \int_h N_e N_H dh = \int_T \text{DEM}(T) dT \quad [\text{cm}^{-5}]$$

EM Loci (see Del Zanna et al. 2002): plot

$$\frac{I_{\text{obs}}}{Ab(Y) G_{ji}(T_e)}$$

Some (significant) results based on approximations have provided incorrect FIP biases.

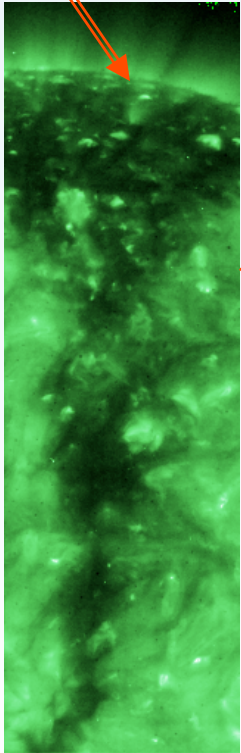


Chemical abundances of coronal hole plumes

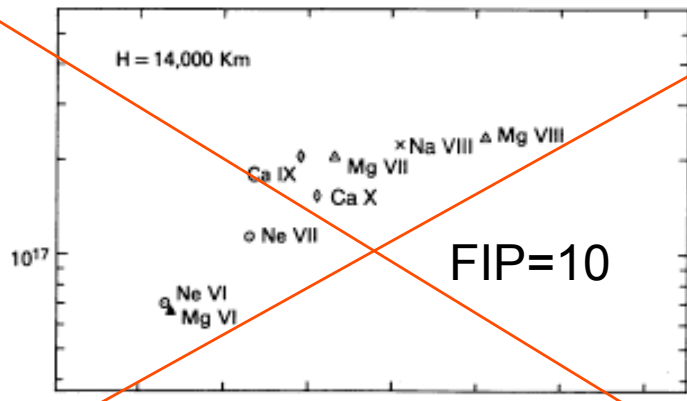
The Widing and Feldman (1989) approximation: the abundances $Ab(X)$ are obtained by imposing a continuous distribution of the values $Ab(X) DEM_L$

FIP effect overestimated by a factor of 10.

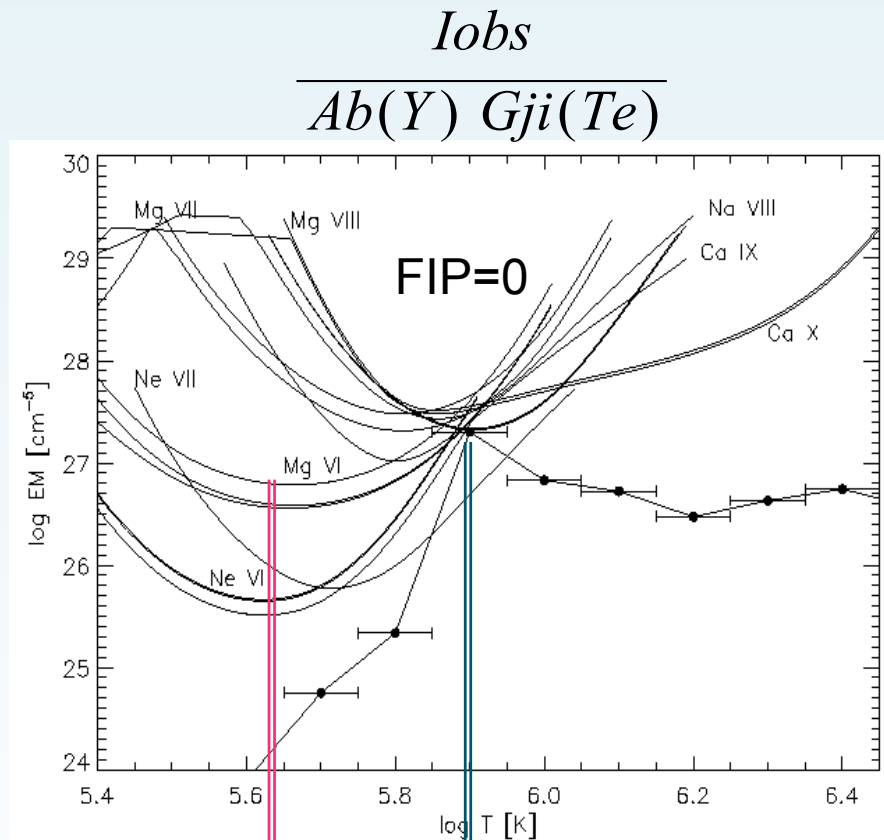
Plumes in coronal holes



$$DEM_L \equiv \frac{I_{ob}}{Ab(X) \int C(T) dT}$$



Widing & Feldman (1992)



Te of maximum emissivity in ionization equilibrium

Actual Te

Del Zanna et al. (2003)

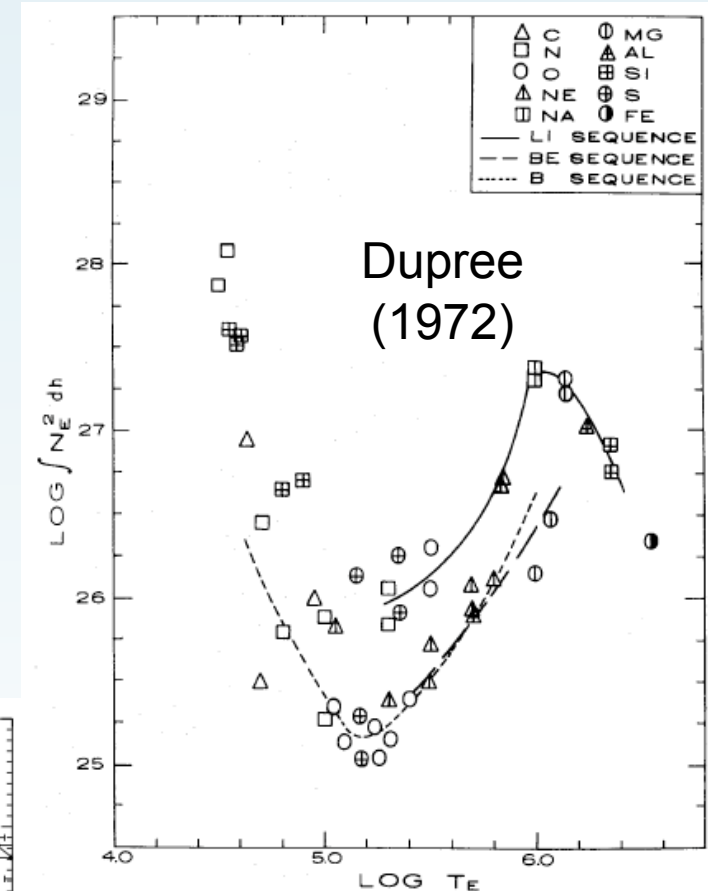
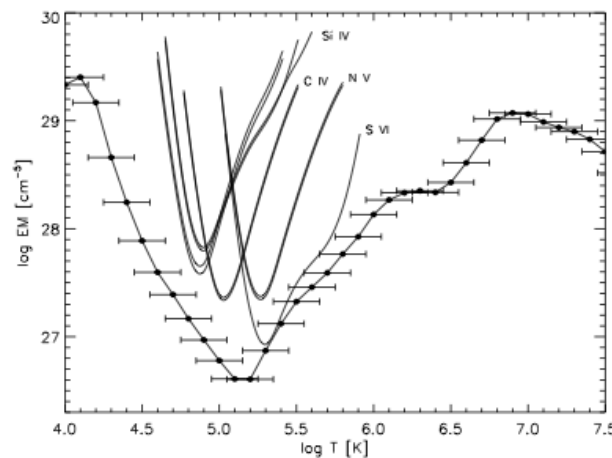
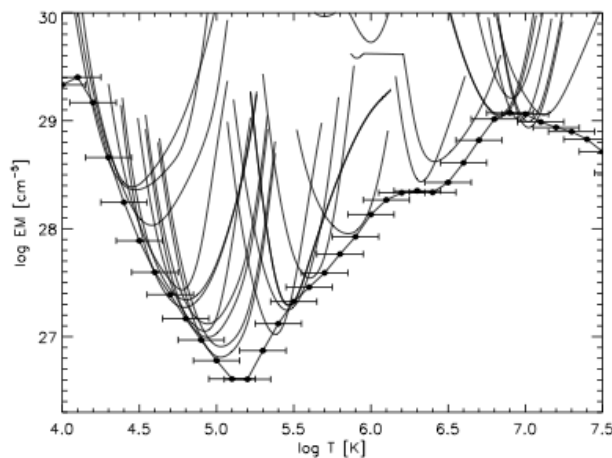
The problem of the 'anomalous' ions

Anomalous EM for lines of the Li and Na isoelectronic sequences (from Burton et al. 1971).

See Del Zanna (1999) and Del Zanna et al. (2001,2002)

Li-like N V and C IV are underestimated by factors of 3 and 10, while those of Ne VIII and Mg X are overestimated by factors of 5 and 10, respectively.

The problem was discovered to apply to stellar coronae by Del Zanna et al. (2002).



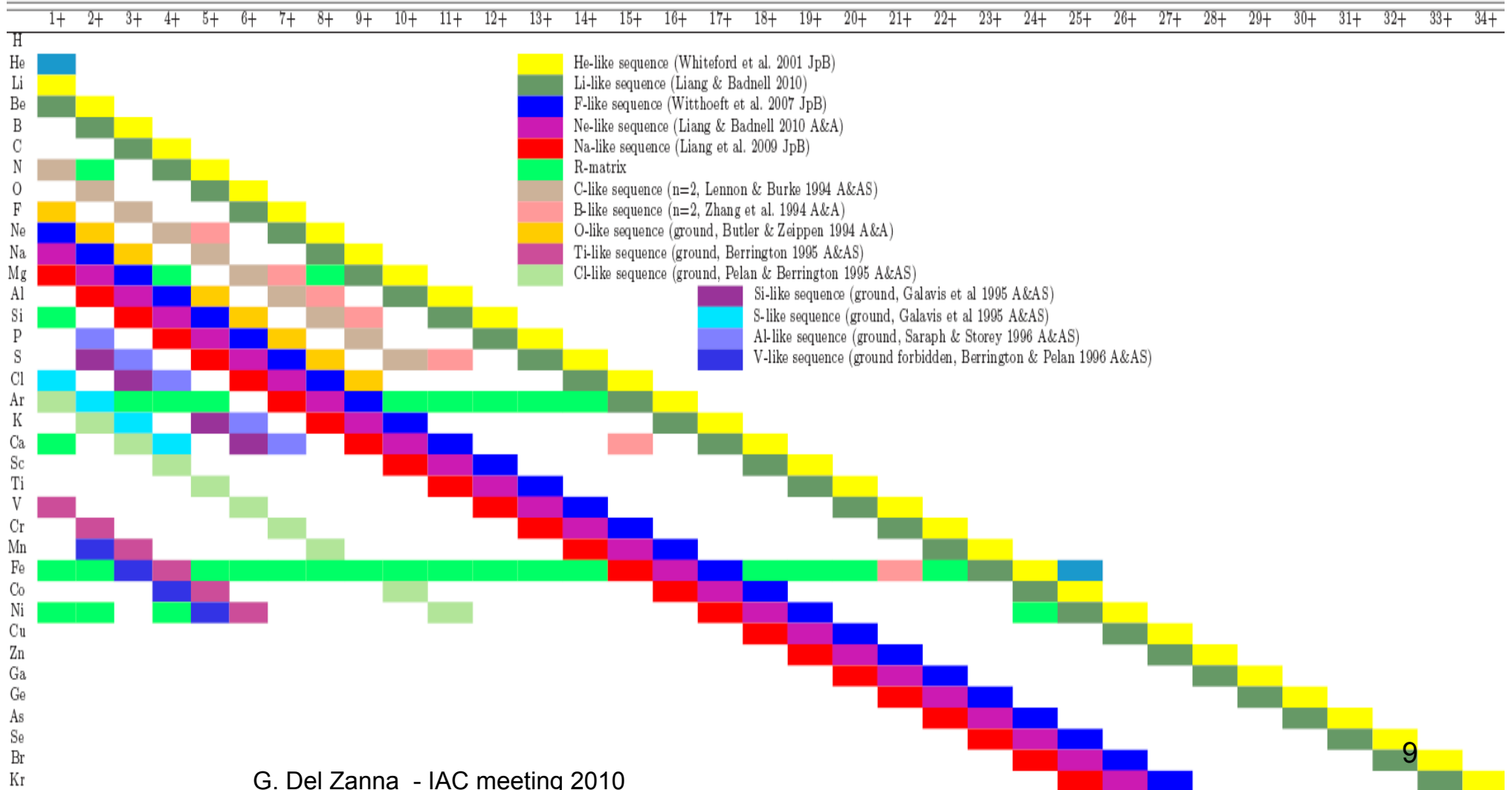
R-matrix data for astrophysically abundant elements

(APAP) : F-like: Witthoef Whiteford Badnell (2007)

Na-like: Liang, Whiteford, Badnell (2009)

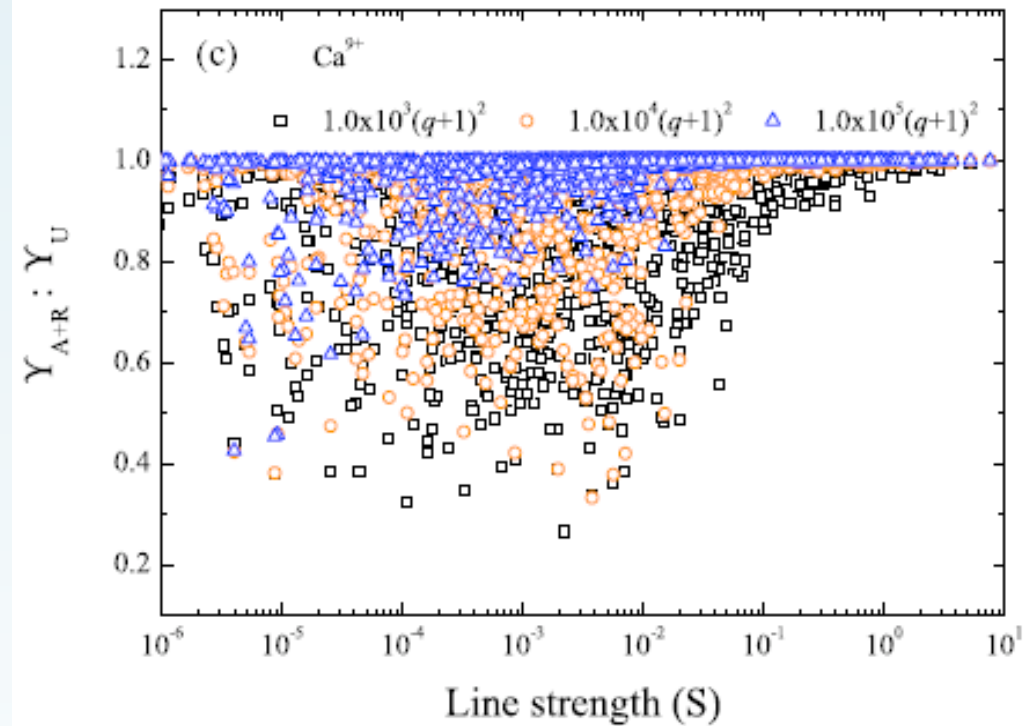
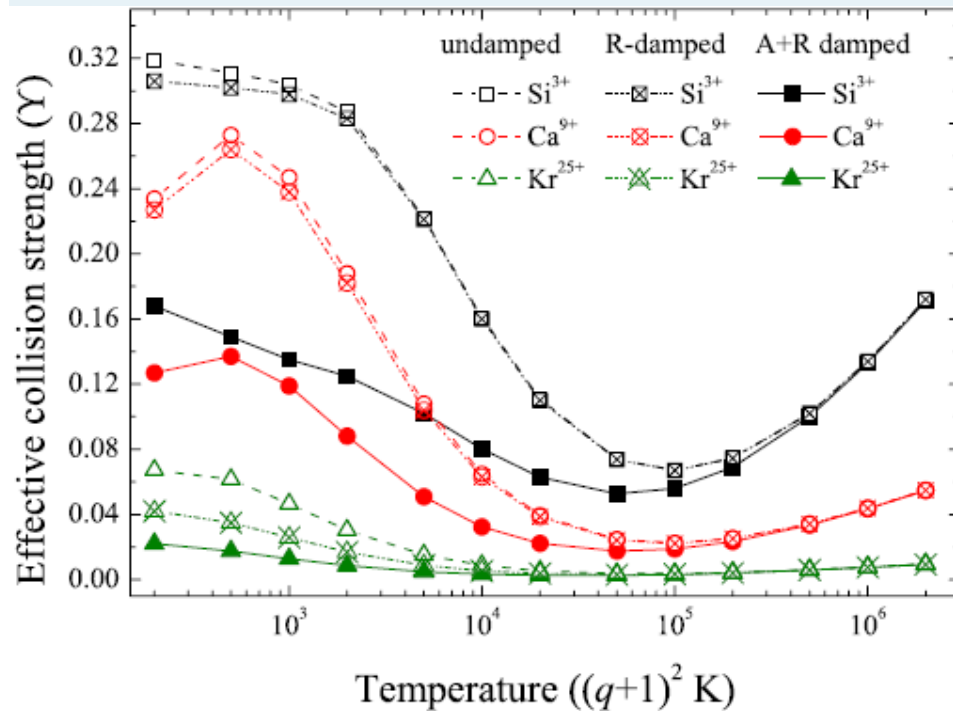
Ne-like: Liang et al. (2010, submitted)

Li-like: Liang & Badnell (2010)



Na-like iso-electronic sequence (valence- and core-excitations)

Liang et al. (2009)

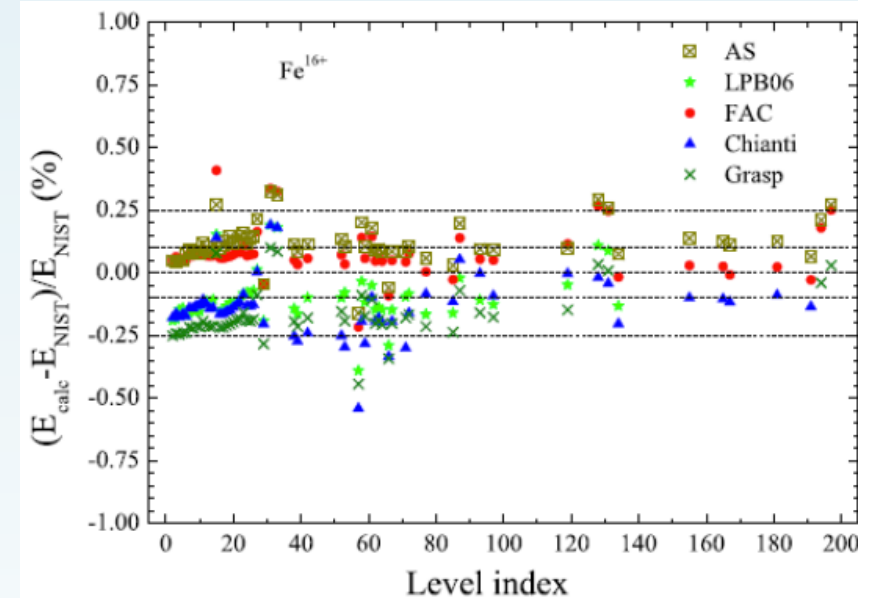
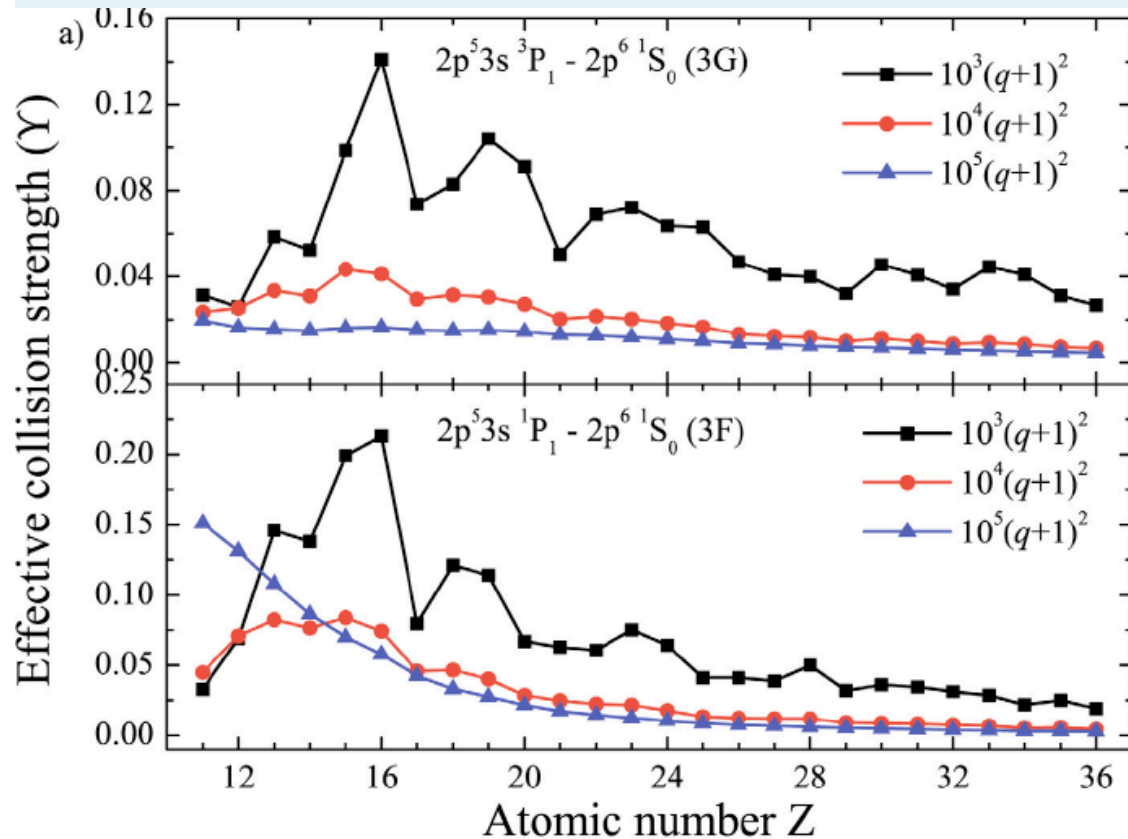


Radiation and Auger damping are included for the core-excitations, and found to be strong and widespread

Complicated structure appears as in cases of F-like and Ne-like sequence for considerable part of transitions

Ne-like iso-electronic sequence

Liang & Badnell (2010a)



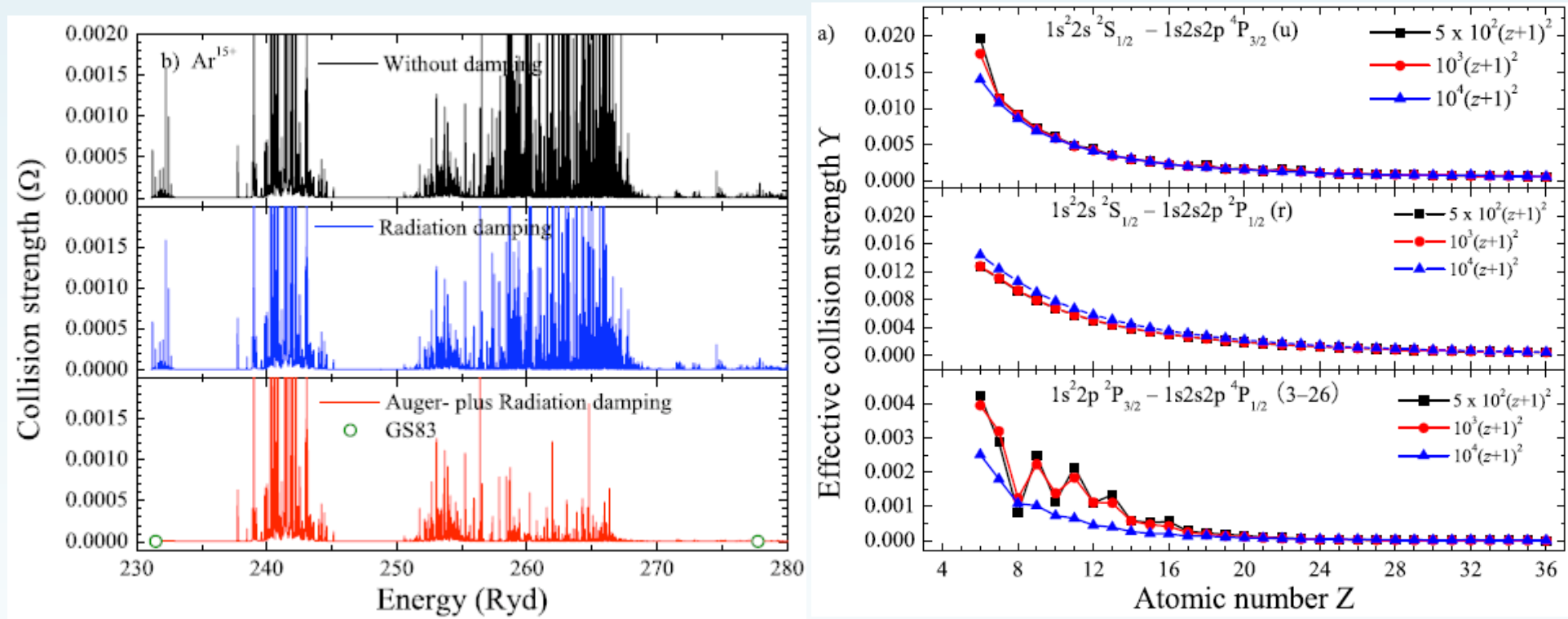
Large-scale calculation with 209 level CC expansions

Detail comparison made to check the accuracy of the sequence calculation

Complicate structure along the sequence appears

Li-like iso-electronic sequence includes core- and valence-excitations

Liang & Badnell (2010b)

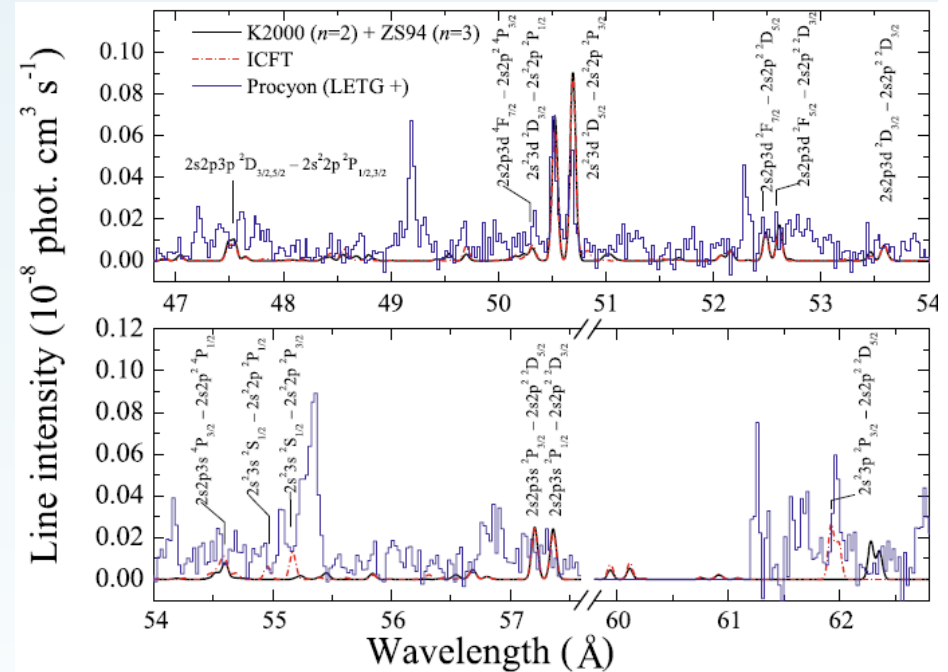
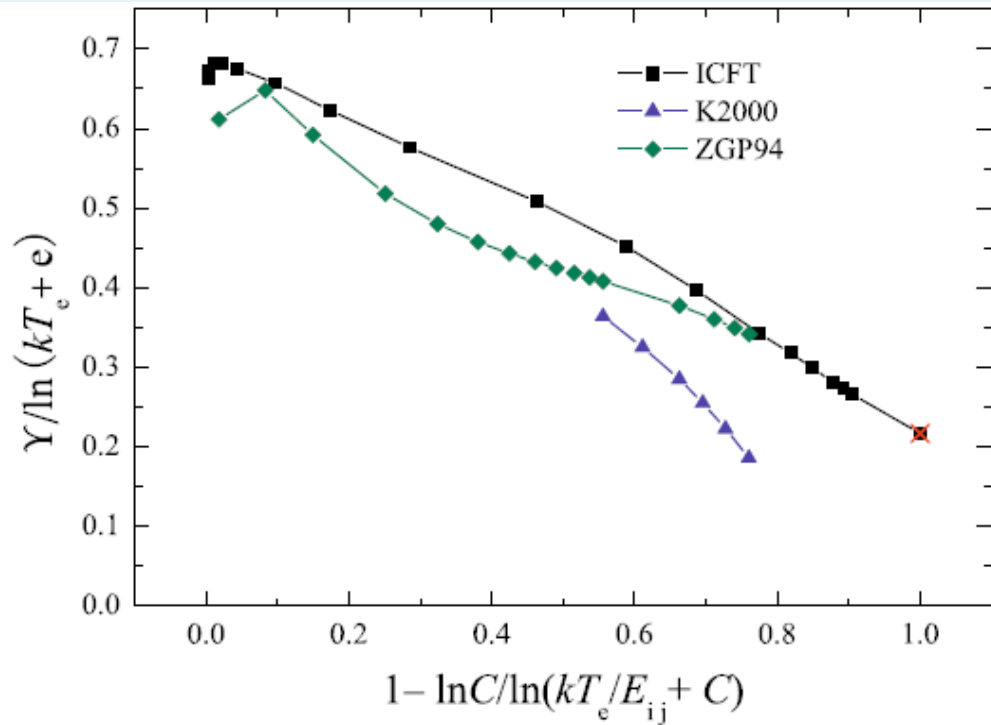


The inclusion of Auger and radiation damping significantly reduce the resonance enhancements

Similar complicate structure appears as other iso-electronic sequence

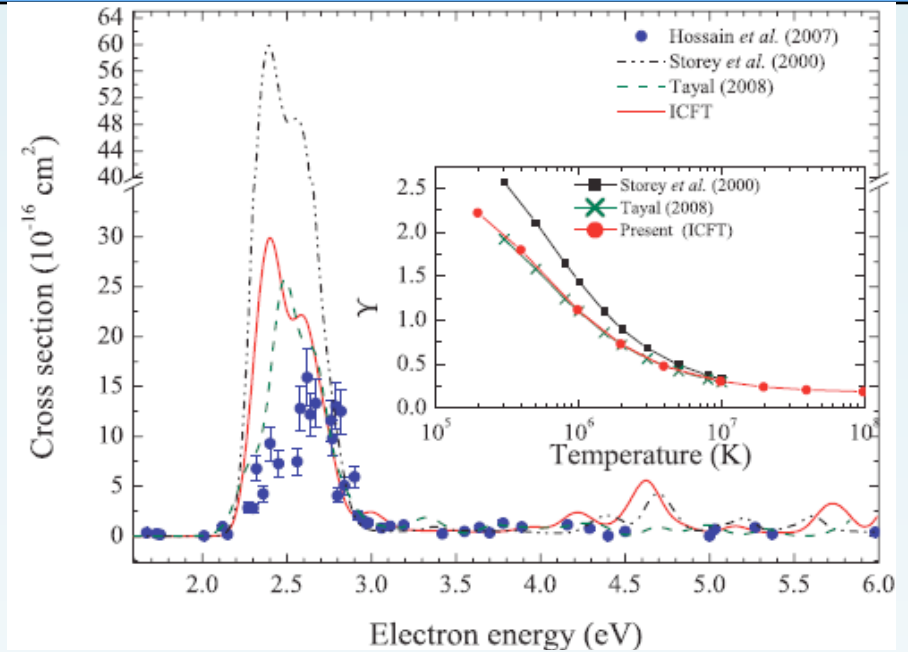
Re-examination for several specific ions (Si^{9+})

An improvement of the excitation data has been made with large-scale model.
 Some new lines are identified with these resultant excitation data
 (Liang et al. 2009)



Re-examination for several specific ions (Fe^{13+})

Liang et al. (2010)



	$\frac{\lambda 220.084}{\lambda 211.317}$	$\frac{\lambda 252.199}{\lambda 264.789}$	$\frac{\lambda 257.394}{\lambda 270.520}$	$\frac{\lambda 289.150}{\lambda 274.203}$	$\frac{\lambda 356.645}{\lambda 334.178}$	$\frac{\lambda 274.203}{\lambda 211.317}$	$\frac{\lambda 334.178}{\lambda 274.203}$	$\frac{\lambda 444.219}{\lambda 334.178}$	$\frac{\lambda 270.520}{\lambda 264.789 + \lambda 274.203}$
Observations									
SERTS-89	0.25 ± 0.07	0.18 ± 0.06	0.38 ± 0.09	0.072 ± 0.024	0.028 ± 0.010	1.01 ± 0.18	0.62 ± 0.10	0.018 ± 0.005	0.24 ± 0.04
BFS08-QS		0.20	0.42	0.040		0.55			0.23
BFS08-AR1		0.18	0.53	0.048		0.46			0.24
BFS08-AR2		0.20	0.62	0.042		0.44			0.22
BFS08-Limb		0.21	0.50	0.054		1.76			0.27
BFS08-Limb + 20''		0.19	0.53	0.040		1.10			0.26
Present-QSoffLimb		0.21 ^a	0.71	0.100 ^b		0.40 ^b			0.23 ^b
Present-AR		0.20 ^a	0.52	0.050 ^b		0.46 ^b			0.26 ^b
Present-high n_e		0.21 ^a	0.54	0.050 ^b		0.46 ^b			0.23 ^b
MH73	0.28	0.26		0.060		0.60			0.26
Laboratory (EBIT) measurements									
$E_e = 325$ eV	0.23 ± 0.07	0.12 ± 0.07^c	0.57 ± 0.14^d			0.49 ± 0.09			0.20 ± 0.03
$E_e = 350$ eV	0.17 ± 0.03	0.20 ± 0.03^c	0.55 ± 0.06^d			0.51 ± 0.08			0.20 ± 0.02
$E_e = 375$ eV	0.15 ± 0.02	0.22 ± 0.03^c	0.61 ± 0.05^d			0.50 ± 0.08			0.19 ± 0.03
$E_e = 400$ eV	0.17 ± 0.02	0.21 ± 0.03^c	0.58 ± 0.04^d			0.51 ± 0.08			0.20 ± 0.02
Theory									
BRS95	0.22	0.23	0.71	0.095	0.038	0.37	0.63		0.35
YLT98	0.21	0.24	0.74	0.089	0.036	0.35 ± 0.03	0.69 ± 0.07	0.015 ± 0.002	
SMY00	0.22	0.24	0.66	0.061	0.029	$0.53^{+0.05}_{-0.03}$	$0.64^{+0.06}_{-0.04}$	$0.028^{+0.011}_{-0.009}$	$0.26^{+0.02}_{-0.01}$
T08	0.21	0.24	0.73	0.091	0.034				
Present	0.21	0.24	0.70	0.076	0.032	0.55	0.70	0.032	0.27

APAP/ADAS adf04 format

Target Energies

SI+	9	14	10	3348008.()
1	2S2	2P1	(2)1(0.5)	0.0
2	2S2	2P1	(2)1(1.5)	7290.0
3	2S1	2P2	(4)1(0.5)	157687.0
4	2S1	2P2	(4)1(1.5)	160324.0
5	2S1	2P2	(4)1(2.5)	164438.0
6	2S1	2P2	(2)2(1.5)	294258.0
7	2S1	2P2	(2)2(2.5)	294455.0
8	2S1	2P2	(2)0(0.5)	375537.0
9	2S1	2P2	(2)1(0.5)	400444.0
10	2S1	2P2	(2)1(1.5)	404878.0

Te

High-E
limit

124	2P2	3D1	(2)2(2.5)	2607801.0												
125	2P2	3D1	(2)2(1.5)	2608628.0												
-1																
10.00	3	2.00+04	5.00+04	1.00+05	2.00+05	5.00+05	1.00+06	2.00+06	5.00+06	1.00+07	2.00+07	5.00+07	1.00+08	2.00+08		
2	1	3.48+00	1.33+00	1.33+00	1.16+00	9.44-01	6.52-01	4.72-01	3.32-01	2.00-01	1.39-01	1.03-01	7.89-02	7.02-02	6.57-02	6.08-02
3	1	3.07+05	3.23-02	3.79-02	3.86-02	3.47-02	2.86-02	2.53-02	2.11-02	1.42-02	9.78-03	6.73-03	4.54-03	3.77-03	3.40-03	1.03-04
4	1	7.24+03	4.45-02	5.78-02	6.01-02	5.38-02	4.37-02	3.86-02	3.21-02	2.11-02	1.40-02	9.17-03	5.64-03	4.34-03	3.66-03	4.63-06

A-value

Rates

Benchmarking atomic data (Del Zanna 2004:)

In a series of papers, I have calculated and benchmarked atomic data for the XUV using a 'novel' approach: atomic structure calculations and comparisons between

- observed and theoretical wavelengths (all brightest lines)
- observed and theoretical line intensities for a wide range of astrophysical and laboratory plasmas using the emissivity ratios:

$$F_{ji}(N_e, T_e) = C \frac{I_{\text{ob}} N_e}{N_j(N_e, T_e) A_{ji}}$$

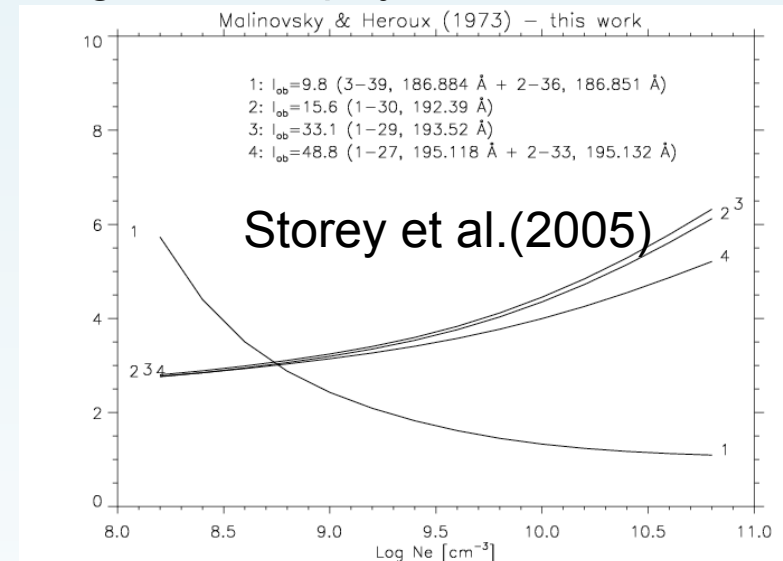
- observed (beam-foil spectroscopy) and theoretical lifetimes and branching ratios.

RESULT:

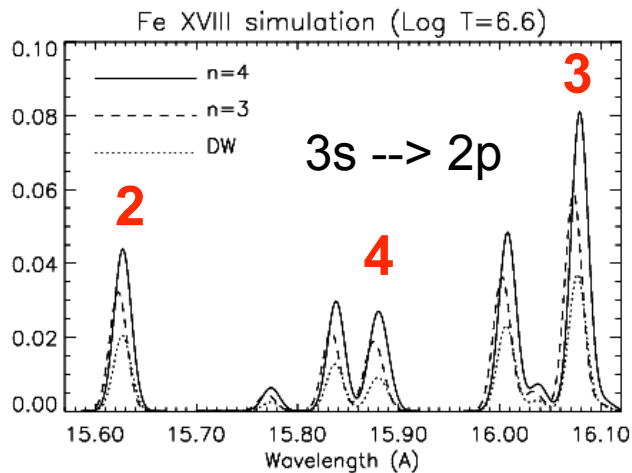
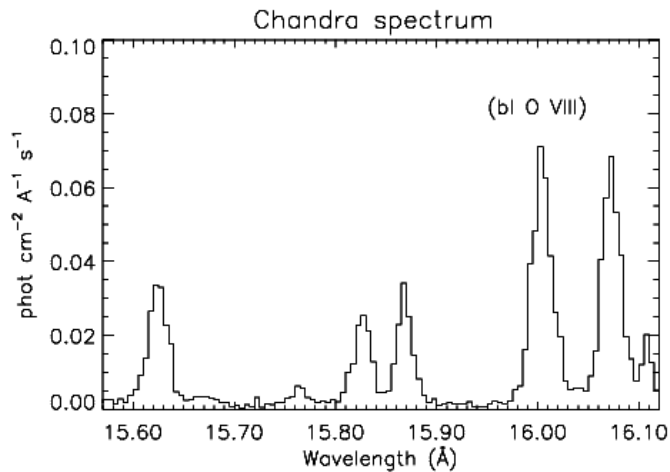
a large number of revised wavelengths (with [uncertainties](#))
new identifications, new level energies (with uncertainties),
new diagnostic applications

For many ions NIST energies are not up-to-date. Not easy to trace original work.

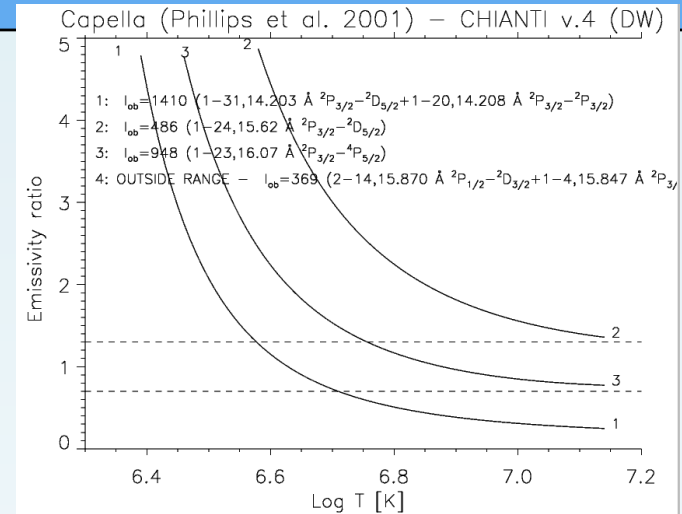
A-values of strongest lines normally accurate to better than 10%
Excitation data normally accurate to better than 20%



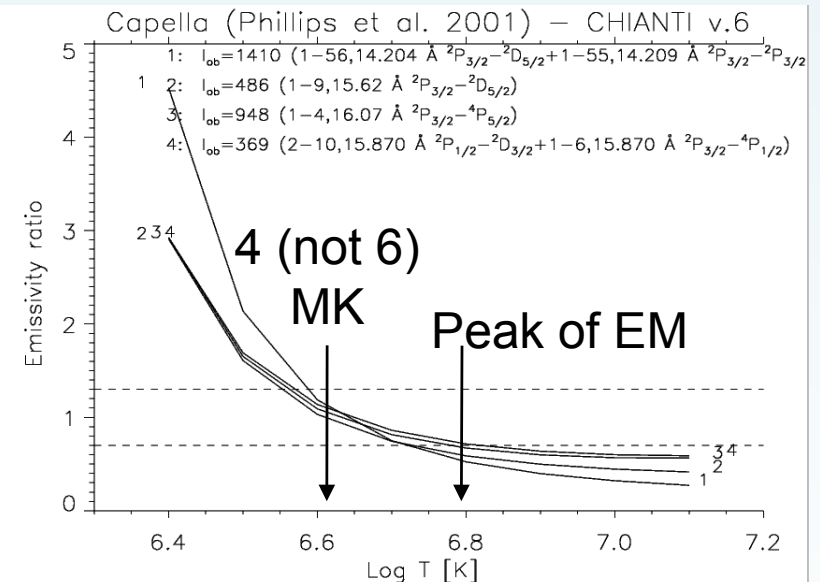
R-matrix ! Fe XVIII



DW:



R-matrix:



The large discrepancies for the strong 3s--> 2p transitions have been resolved with the first R-matrix e- scattering calculation by Witthoeft, Badnell, Del Zanna et al. (2006).

New diagnostics to measure electron temperatures and densities (Del Zanna 2006).

Fe XI – 6 years !

Atomic Data from the IRON Project

LXVIII. Electron impact excitation of Fe XI^{*}

G. Del Zanna¹, P.J. Storey², and H.E. Mason¹

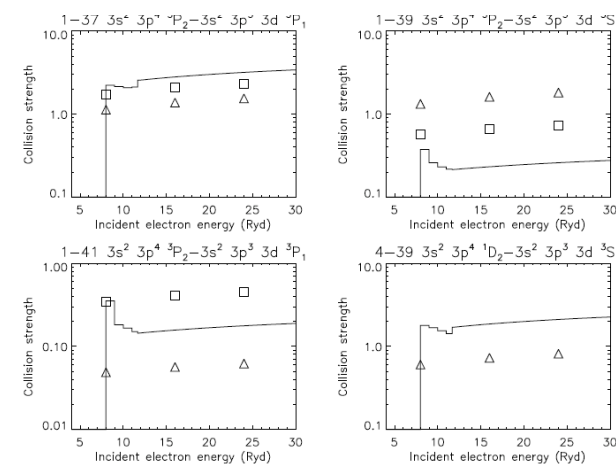
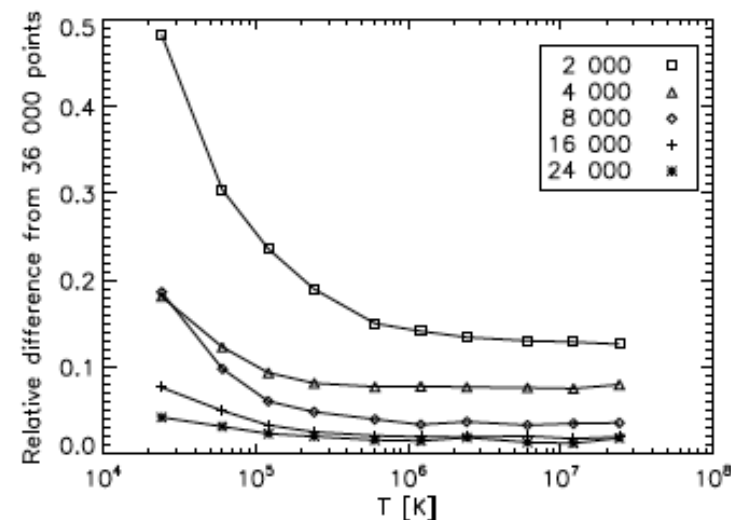


Fig. 7. Collision strengths for transitions involving the three $J = 1$ levels, averaged over 1 Ryd. Boxes indicate the GT99 values, while triangles the AK03 ones.



i	Conf.	Lev.	E_{exp}	E_{NIST}	E_{bench}	E_{bench} (TEC)	$E_{\text{MR-MP}}$
1	$3s^2 3p^4$	3P_2	0	0	0	0	0
2	$3s^2 3p^4$	3P_1	12667	12667 (0)	12371 (297)	12397 (271)	12667 (0)
3	$3s^2 3p^4$	3P_0	14306	14312 (-6)	14283 (23)	14155 (151)	14312 (-6)
4	$3s^2 3p^4$	1D_2	37743	37743 (-1)	38324 (-581)	37748 (-5)	37743 (-1)
5	$3s^2 3p^4$	1S_0	80831	80814 (16)	83640 (-2809)	80842 (-11)	80814 (16)
6	$3s 3p^5$	3P_2	283551	283558 (-7)	283764 (-213)	283658 (-107)	283739 (-188)
7	$3s 3p^5$	3P_1	293158	293158 (0)	293229 (-71)	293089 (69)	293315 (-157)
8	$3s 3p^5$	3P_0	299163	299163 (0)	299059 (104)	298953 (210)	299308 (-145)
9	$3s 3p^5$	1P_1	361846	361842 (4)	365012 (-3166)	361678 (168)	361675 (171)
10	$3s^2 3p^3 3d$	5D_0	387544	-	389671 (-2127)	387427 (117)	387622 (-78)
11	$3s^2 3p^3 3d$	5D_1	387726	-	389870 (-2144)	387628 (98)	387811 (-85)
12	$3s^2 3p^3 3d$	5D_2	387940	-	390118 (-2178)	387866 (74)	388020 (-80)
13	$3s^2 3p^3 3d$	5D_3	388268	-	390506 (-2238)	388236 (32)	388335 (-67)
14	$3s^2 3p^3 3d$	5D_4	389227	-	391510 (-2283)	389244 (-17)	389274 (-47)
15	$3s^2 3p^3 3d$	3D_2	412856	-	416494 (-3638)	413082 (-226)	412968 (-112)
16	$3s^2 3p^3 3d$	3D_3	415426	-	418774 (-3348)	415618 (-192)	415477 (-51)
17	$3s^2 3p^3 3d$	3D_1	417049	-	420300 (-3251)	417205 (-156)	417139 (-90)
18	$3s^2 3p^3 3d$	3F_4	422844	-	426701 (-3857)	422557 (287)	422920 (-76)
19	$3s^2 3p^3 3d$	1S_0	-	-	428625	425466	425465
20	$3s^2 3p^3 3d$	3F_3	426022	-	429980 (-3958)	425712 (310)	426149 (-127)
21	$3s^2 3p^3 3d$	3F_4	430522	-	434444 (-3922)	430102 (420)	430589 (-67)
22	$3s^2 3p^3 3d$	3G_3	-	-	453512	448623	448615
23	$3s^2 3p^3 3d$	3G_2	450211	-	455092 (-4881)	450218 (-7)	450228 (-17)
24	$3s^2 3p^3 3d$	3G_4	452416	-	457218 (-4802)	452414 (2)	452413 (3)
25	$3s^2 3p^3 3d$	1G_0	459218	-	464621 (-5403)	459220 (-2)	459231 (-13)
26	$3s^2 3p^3 3d$	1D_2	-	-	472489	466545	466458
27	$3s^2 3p^3 3d$	3D_1	-	-	488110	481678	481722
28	$3s^2 3p^3 3d$	3P_0	-	-	488573	482071	482618
29	$3s^2 3p^3 3d$	3P_1	484830	-	491259 (-6429)	484676 (154)	484990 (-160)
30	$3s^2 3p^3 3d$	3F_2	485039	-	491500 (-6461)	485125 (-86)	485081 (-42)
31	$3s^2 3p^3 3d$	3F_3	-	-	492645	486234	486227
32	$3s^2 3p^3 3d$	3F_4	486413	-	492671 (-6258)	486445 (-32)	486412 (1)
33	$3s^2 3p^3 3d$	3D_2	489378	-	495788 (-6410)	489376 (2)	489528 (-150)
34	$3s^2 3p^3 3d$	3P_2	494013	496090 (-2077)	500566 (-6553)	494055 (-42)	494053 (-40)
35	$3s^2 3p^3 3d$	3D_3	497235	-	503664 (-6429)	497216 (19)	497452 (-217)
36	$3s^2 3p^3 3d$	1F_3	525260	-	532842 (-7582)	525278 (-18)	525332 (-72)
37	$3s^2 3p^3 3d$	$^3P_1^{\circ}$	531070	526480 (4590)	540265 (-9195)	530770 (300)	531839 (-769)
38	$3s^2 3p^3 3d$	$^3P_2^{\circ}$	531304	531290 (14)	541300 (-9996)	531551 (-247)	531502 (-198)
39	$3s^2 3p^3 3d$	$^3S_1^{\circ}$	533445	533450 (-5)	543921 (-10476)	533838 (-393)	533343 (102)
40	$3s^2 3p^3 3d$	$^3P_0^{\circ}$	541777	541720 (57)	551873 (-10096)	542143 (-366)	541892 (-115)
41	$3s^2 3p^3 3d$	$^3P_1^{\circ}$	541424	541390 (34)	551800 (-10376)	541729 (-305)	541178 (246)
42	$3s^2 3p^3 3d$	3D_3	554321	554300 (21)	564972 (-10651)	554308 (13)	554305 (16)
43	$3s^2 3p^3 3d$	3D_1	561615	561610 (5)	572350 (-10735)	561671 (-56)	561556 (59)
44	$3s^2 3p^3 3d$	3D_2	566396	566380 (16)	577055 (-10659)	566321 (75)	566299 (97)
45	$3s^2 3p^3 3d$	1D_2	578890	578860 (30)	589847 (-10957)	578887 (3)	578539 (351)
46	$3s^2 3p^3 3d$	1F_3	594047	594030 (17)	605953 (-11906)	594047 (0)	594518 (-471)
47	$3s^2 3p^3 3d$	1P_1	623101	623080 (21)	636559 (-13458)	623094 (7)	623252 (-151)
48	$3p^6$	1S_0	-	-	625608	614643	-

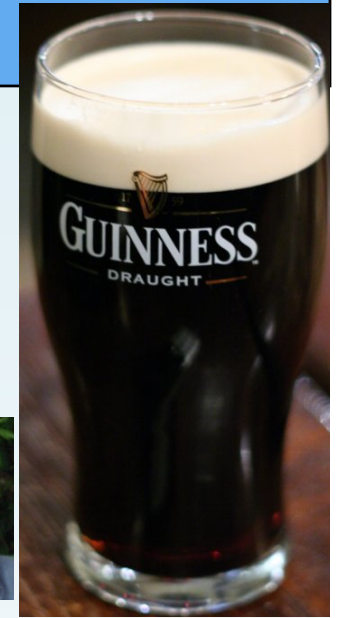
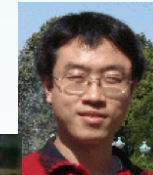
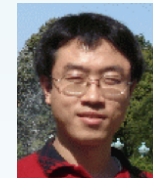
Table 3. Summary of line identifications for Fe xi.

Del Zanna (2010)

<i>i-j</i>	λ_{exp} (Å)	λ_{obs} (Å)	ID	Diff. ID
6-103	168.929	? 168.929(10) Be76	N	
1-43	178.058	178.056(4) Be76	G66	
4-46	179.758	179.758(10) Be76	G66	
1-42	180.401	180.401(2) Be76 (bl)	G66	
2-44	180.594	180.595(4) Be76	F71	
3-44	181.130	181.131(10) Be76	G66	
2-43	182.167	182.167(2) Be76	G66	
4-45	184.793	184.793(10) Be76 (bl u)	FG66	
1-38	188.216	188.216(2) Be76	B77	F71 (188.299)
1-37	188.299	188.299(2) Be76	J93	B77(189.94)
2-41	189.123	189.123(4) Be76 (bl u)	B77	J93 (192.619)
3-41	189.711	189.723(5) N (bl)	B77	
1-36	190.382	190.382(5) N (bl u)	N	Be76 (S xi)
2-39	192.021	192.021(5) N (bl)	B77	
3-39	192.627	192.624(5) N (bl u)	B77	
2-38	192.813	192.811(5) N (bl O v, u)	F71	
3-37	193.512	- (bl Fe xii 193.509(2))		
4-41	198.538	198.555(10) Be76 (bl S viii)	B77	Be76, J93
1-35	201.112	201.112(5) N (bl Fe xiii)	N	
4-39	201.734	201.734(10) Be76 (bl Fe xii)	B77	
1-34	202.424	202.424(10) Be76 (bl u)	N	B77 (201.575)
4-38	202.609	- (bl S viii 202.608(10))		
4-37	202.705	202.710(10) Be76 (bl)		
1-30	206.169	206.169(10) Be76 (bl u)	N	
1-29	206.258	206.258(5) N	N	
2-34	207.751	207.749(5) N (bl u)	N	
2-33	209.771	209.771(5) N (bl u)		
1-20	234.730	234.73(2) D78	N	D78 (Fe xv)
1-18	236.494	236.494(10) Be76	N	
1-17	239.780	? 239.78(2) D78	N	
1-16	240.717	240.713(4) Be76 (bl Fe xiii)	N	
1-15	242.215	242.215(10) (bl) Be76	N	
4-21	254.596	254.600(5) N	N	
1-14	256.919	256.925(5) N (bl Fe xii)	N	
4-20	257.547	257.547(10) Be76 (sbl)	N	
1-13	257.554	257.547(10) Be76 (sbl)	J93	T98 (257.26 T)
1-12	257.772	257.772(4) Be76	J93	T98 (257.55 T)
1-11	257.914	257.914(5) N	N	T98 (257.78 T)
4-16	264.772	bl Fe xiv 264.787	N	
4-15	266.586	? 266.613(5) N (bl)	N	
21-79	266.759	266.755(5) N (bl u)	N	

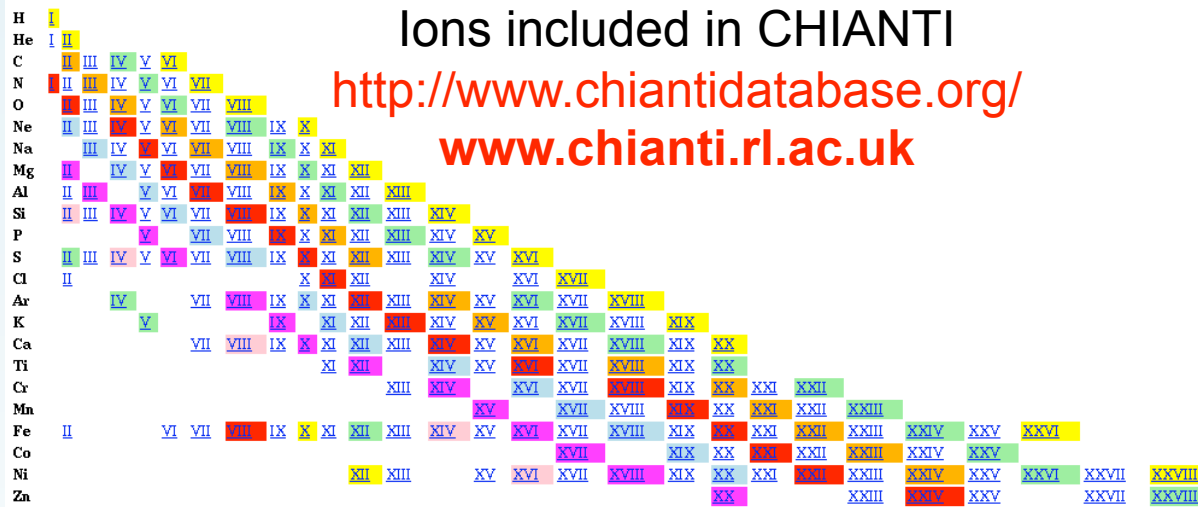
Good things come to those who wait...

- Fe VII: Witthoeft et al. (2008) S
Del Zanna (2010) ID
- Fe VIII: Griffin et al. (2000) S
Del Zanna (2010) ID
- Fe IX: Storey et al. (2002) S
- Fe X: Del Zanna, Berrington, Mason (2004) S, ID
- Fe XI: Del Zanna, Storey, Mason & Del Zanna 2010 S, ID
- Fe XII: Storey et al. 2005 (S); Del Zanna & Mason (2005) S, ID
- Fe XIII: Storey & Zeppen (2010) S
- Fe XIV: Storey et al. (2000); Liang et al. (2010) S
- Fe XV Berrington et al. (2005)
- Fe XVII: Loch et al. (2006), Liang et al. (2010).
ID: Del Zanna & Ishikawa (2009).
- Fe XVIII: Witthoeft et al.(2006). Del Zanna (2006).
- Fe XX: Witthoeft, Del Zanna, Badnell (2007)
- Fe XXIII Chidichimo et al. (2005) S; Del Zanna et al. (2005) ID
- Fe XXIV Whiteford et al. (2002) S; Del Zanna (2006) ID



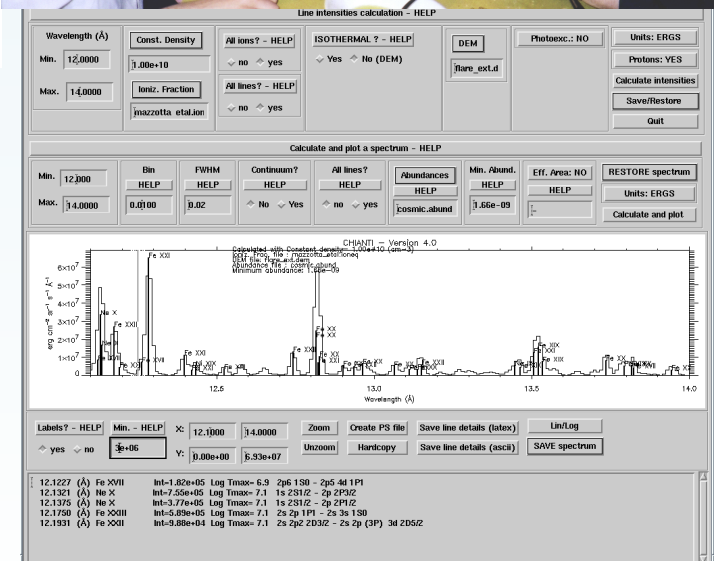
CHIANTI atomic package

CHIANTI Provides all atomic data and IDL programs necessary for modelling spectra from collisionally-ionised plasmas for the XUV. Over 1000 citations.
User base: solar physics, astrophysics, X-ray, EUV, UV



V.6 released (Dere et al.2009) contains **new atomic data and new ionization and recombination rates**

Basic atomic data from e.g. CHIANTI are included in many other spectral codes. Photoionization (XSTAR, CLOUDY, MOCASSIN) and others (ATOMDB, XSPEC, ISIS, PINTofALE).



CHIANTI data (ascii)



fe_12.elvlc	Energy levels (theoretical, observed), LSJ for Fe XII (Fe ¹¹⁺)
fe_12.wgfa	Transition probabilities, gf values, theoretical, observed wavelengths
fe_12.splups	spline fits to Maxwellian-averaged e ⁻ collision strengths in Burgess & Tully (1992) scaled domain. Each transition is assessed. Data from IP, APAP-Network, literature.
fe_12.psplus	Same but for protons.
.diparams .drparams .rrparams	DI, DR, RR total rates

Version 7 (2010) – same format
Version 8 – new format

slider: low Ups value
36

slider: Hi Ups value

line 6 (10153 lines)
lvl1: 3s2 3p3 4S3/2
lvl2: 3s 3p4 4P3/2
gf= 1.3e-01

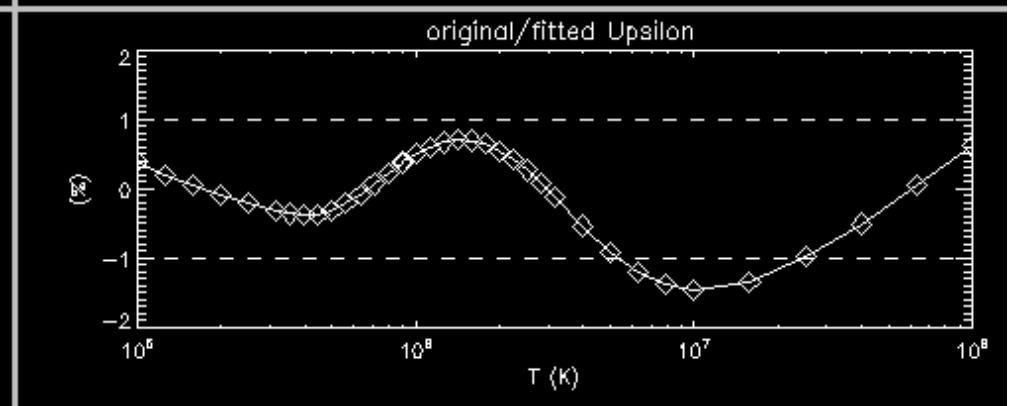
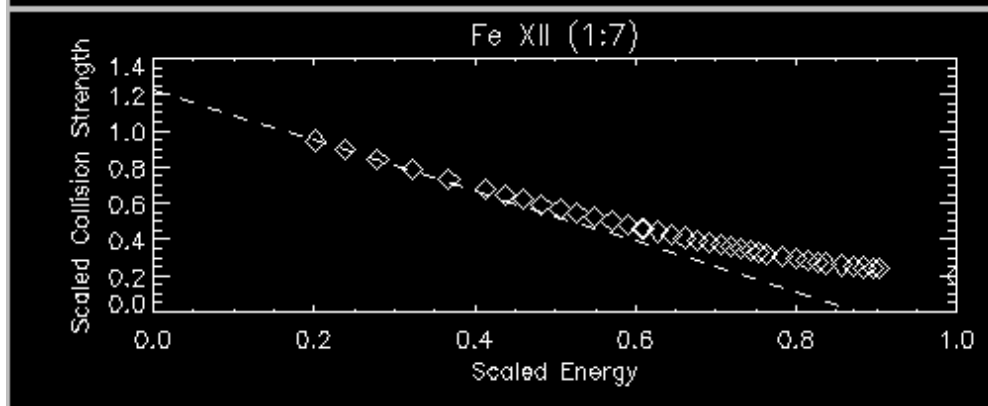
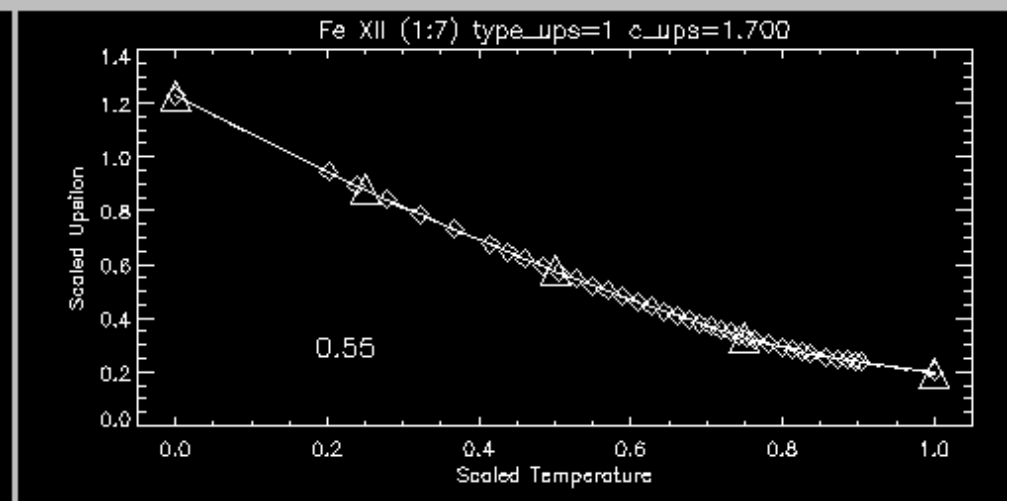
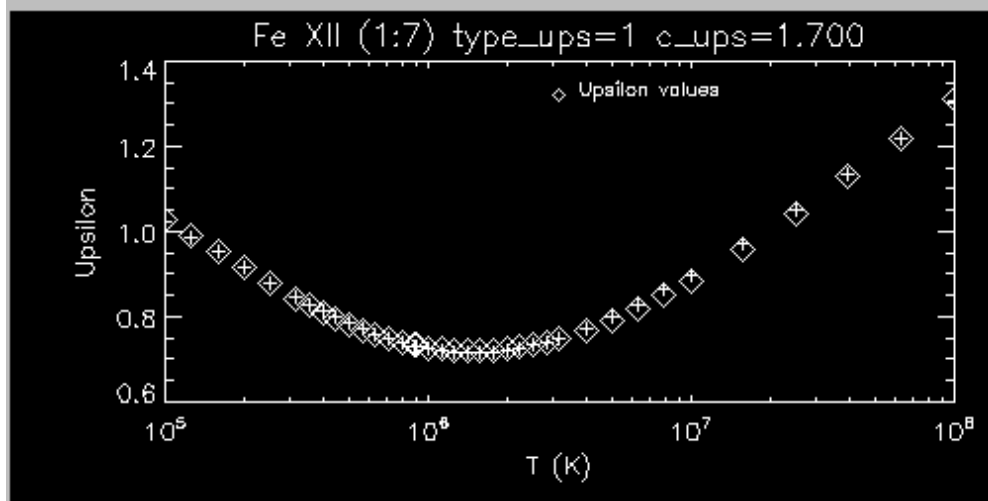
Extrapolate to 1
Spline Fit
\$UPS(0)=1.228 \$UPS(1)= 0.097
Undo Extrap
 Choose extrap points?
ex1: 0
ex2: 36

x10 x1.0 /10
0
c = 10. * value
1
c = 1.0 * value
7
c = 0.1 * value
c_ups= 1.70

Output Data + step 1
Autom. Output Data
Create PS File
EXIT

slider lower level lvl1
7
slider upper level lvl2

JPS = Dipole (1)
UPS = Forbidden (2)
UPS = Intercomb (3)
UPS = Dipole sm gf (4)




Normally we include only e excitation rates from ground state and to/from metastable levels. Valid until electron densities of 10^{14} cm^{-3} or so for many ions.

CHIANTI emissivities are currently calculated for plasmas in ionization equilibrium.

There are ways to estimate emissivities for non-Maxwellian electrons

CHIANTI data and programs are distributed via

- + a tar file (www)
- + SolarSoft (IDL packages for Solar Physics).
- + (testing phase) Python interface (www)

The logo for ChiantiPy features the word "ChiantiPy" in a large, red, stylized font. The "i" in "Py" is notably larger and more decorative. To the right of this, the text "The Python interface to the CHIANTI atomic database for astrophysical spectroscopy" is written in a smaller, red, sans-serif font.

ChiantiPy The Python interface to the CHIANTI atomic database for astrophysical spectroscopy

Collisions with photons

Photoexcitation and stimulated emission Not important in the very low corona. However, at densities of about 10^7 starts to become important. It is also very important for the infrared forbidden lines and any low-density plasma not far from a strong source of photons (as a planetary nebula).

The generalised photon rate coefficient for a Maxwellian distribution is:

$$A_{ij} = \begin{cases} W(R) A_{ji} \frac{\omega_j}{\omega_i} \frac{1}{\exp(\Delta E/kT_*) - 1} & i < j \\ A_{ji} \left[1 + W(R) \frac{1}{\exp(\Delta E/kT_*) - 1} \right] & i > j \end{cases}$$

Where W is the radiation dilution factor which accounts for the weakening of the radiation field at distance. Within CHIANTI, a uniform spherical source of black-body radiation is assumed by default. However, user-defined radiation fields can be specified.

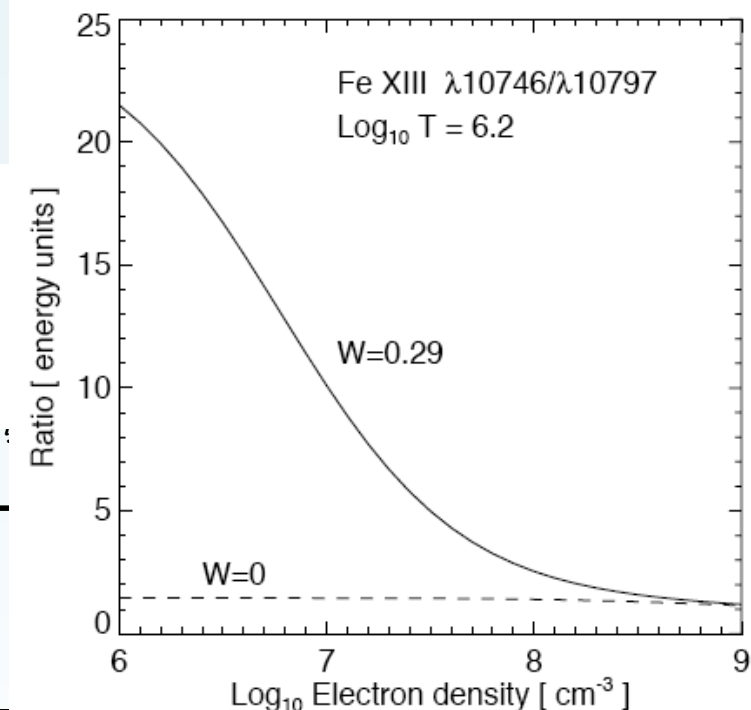


FIG. 3.—Fe XIII $\lambda 10746/\lambda 10797$ ratio plotted as a function of density for two different dilution factors. $W = 0$ corresponds to no radiation field, while $W = 0.29$ corresponds to 0.1 source radii above the source surface ($r_* = 1.1$).

CHIANTI v.3

CHIANTI & Astrogrid (VO) - 2006

- CHIANTI data were imported into a MySQL database.

Tables: SpectralLines and LineEmissivities. Link to the VO:

1. using ESAC DAL Toolkit to install a SLAP server (DMMapper can translate from CHIANTI data model to Line data model)
Data appear automatically in VOSpec, once registered. -
2. by means of **AstroGrid**: www2.astrogrid.org DSA software: user can build ADQL queries on the CHIANTI tables via Workbench.

Spectral Lines table

Result of query to spectral lines table via AstroGrid DSA:

TOPCAT(1): Table Browser

File Subsets Help

Table Browser for 1: votable

	LINE_NUM...	CHEMIC...	IONISAT...	TITLE	FINAL_L...	INITIAL...	TRANSI...	WAVELENGTH_METE...	THEORETICAL...	WEIGHTED_O...	EINSTEIN_A	FINAL...
1	183728	26	14	Fe XV 180.0108 A	154	267	2	1.80011E-8	1.80011E-8	0.5414	1.59200E10	3 d 4
2	17160	26	22	Fe XXIII 180.0180 A	15	36	1	1.80018E-8	1.81598E-8	0.	727.3	2 s 3
3	201205	26	8	Fe IX 180.0318 A	11	106	2	1.80032E-8	1.80032E-8	1.935	5.68600E10	3 s 2
4	191364	26	11	Fe XII 180.0329 A	10	105	2	1.80033E-8	1.80033E-8	0.000879	2.79900E7	3 s 3
5	197329	26	9	Fe X 180.0382 A	35	84	2	1.80038E-8	1.80038E-8	0.289	8.60800E9	3 s 3
6	16620	26	22	Fe XXIII 180.0400 A	4	7	1	1.80040E-8	1.80481E-8	0.06407	4.39500E9	2 s 2
7	168282	26	17	Fe XVIII 180.0506 A	196	238	2	1.80051E-8	1.80051E-8	0.001184	6.09200E7	2 s 2
8	48765	26	21	Fe XXII 180.0554 A	154	212	2	1.80055E-8	1.80055E-8	0.04897	5.03800E9	2 s 2
9	186344	28	14	Ni XV 180.0558 A	3	23	1	1.80056E-8	1.75817E-8	0.2433	1.66900E10	3 s 2
10	1147	15	14	P XV 180.0569 A	14	19	1	1.80057E-8	1.80008E-8	0.1671	8.58900E9	4 d
11	183746	26	14	Fe XV 180.0604 A	155	268	2	1.80060E-8	1.80060E-8	3.244	7.41500E10	3 d 4
12	183857	26	14	Fe XV 180.0623 A	161	281	2	1.80062E-8	1.80062E-8	0.008523	3.50700E8	3 p 5
13	116151	26	19	Fe XX 180.0665 A	355	473	2	1.80067E-8	1.80067E-8	0.007767	7.98900E8	2 s 2
14	118329	26	19	Fe XX 180.0710 A	627	703	2	1.80071E-8	1.80071E-8	0.03371	1.15600E9	2 s 2
15	183696	26	14	Fe XV 180.0710 A	152	253	2	1.80071E-8	1.80071E-8	0.1018	1.90400E9	3 d 4
16	187740	26	11	Fe XII 180.0783 A	5	47	2	1.80078E-8	1.80078E-8	0.	9248.	3 s 2
17	194770	26	11	Fe XII 180.0926 A	22	140	2	1.80093E-8	1.80093E-8	0.5435	1.75700E10	3 s 2
18	200097	26	9	Fe X 180.0928 A	86	168	2	1.80093E-8	1.80093E-8	0.00157	1.59000E8	3 s 2
19	200139	26	9	Fe X 180.0928 A	86	169	2	1.80093E-8	1.80093E-8	0.001221	6.18200E7	3 s 2
20	195445	28	12	Ni XIII 180.0948 A	2	34	2	1.80095E-8	1.80095E-8	0.03633	1.49400E9	3 s 2
21	27975	10	5	Ne VI 180.0997 A	12	40	1	1.80100E-8	1.80043E-8	3.67800E-6	3.78000E5	2 p 3
22	183745	26	14	Fe XV 180.1148 A	155	267	2	1.80115E-8	1.80115E-8	0.02654	7.79600E8	3 d 4
23	169495	18	8	Ar IX 180.1250 A	15	55	1	1.80125E-8	1.75766E-8	0.02555	1.75000E9	2 s 2
24	117906	26	19	Fe XX 180.1342 A	554	654	2	1.80134E-8	1.80134E-8	0.00568	1.94600E8	2 s 2
25	117916	26	19	Fe XX 180.1339 A	556	657	2	1.80134E-8	1.80134E-8	0.0435	2.23500E9	2 s 2
26	56793	16	10	S XI 180.1361 A	45	49	2	1.80136E-8	1.80136E-8	0.	42.	2 s 2
27	180762	26	14	Fe XV 180.1361 A	42	107	2	1.80136E-8	1.80136E-8	0.00119	2.44600E8	3 s 4
28	201196	26	8	Fe IX 180.1386 A	11	105	2	1.80139E-8	1.80139E-8	0.08465	3.47800E9	3 s 2
29	118115	26	19	Fe XX 180.1445 A	586	674	2	1.80144E-8	1.80144E-8	0.4235	7.25400E9	2 s 2
30	118114	26	19	Fe XX 180.1480 A	586	673	2	1.80148E-8	1.80148E-8	0.01876	4.81900E8	2 s 2
31	75807	26	20	Fe XXI 180.1489 A	415	539	2	1.80149E-8	1.80149E-8	0.01088	4.47100E8	2 s 2
32	181504	26	14	Fe XV 180.1486 A	64	170	2	1.80149E-8	1.80149E-8	0.004342	1.78500E8	3 p 4
33	86746	20	13	Ca XIV 180.1600 A	11	15	1	1.80160E-8	1.76078E-8	0.000137	1.41200E7	2 s 2

- WP4 SA1 Giulio Del Zanna & Helen Mason (DAMTP, Univ. of Cambridge)
- Collaboration with IoA (Nic Walton, Guy Rixon)
- MSSL, UCL (Len Culhane, Kevin Benson, Peter Kuen)

- **BASIC DATA**: first table: wavelength, A-value, gf-value, configuration, LSJ, observed, theoretical energy of upper and lower levels.
To do: add other basic atomic data (rates).
Maintain identity of each database.
Problem of multiple calculations. CHIANTI policy is to select one.
Problem of upgrades (main once every 1-2 years)
Essential to provide **appropriate references to original calculation in the literature ! Not simple to transfer info.**

- **DERIVED DATA (modelling)**: second table: line emissivities in a grid of temperatures and densities.
- **To do: write simple scripts to call CHIANTI routines via the MSSL server (IDL and CHIANTI installed). Alternatively, write Python programs.**

END

Thank you !